Ab initio molecular dynamics simulated annealing at the generalized valence bond level. Application to a small nickel cluster

Bernd Hartke

Department of Chemistry, University of Bielefeld, Universitätsstrasse 25, D-33615 Bielefeld, Germany

and

Emily A. Carter

Department of Chemistry and Biochemistry, University of California, 405 Hilgard Avenue, Los Angeles, CA 90024-1569, USA

Received 28 August 1993; in final form 26 October 1993

The feasibility of ab initio generalized valence bond molecular dynamics simulated annealing for applications to small systems of realistic complexity is demonstrated by the successful location of the global energy minimum on the potential energy surface of $^2Ni_5$, independent of the initial conditions.

1. Introduction

In recent years, ab initio molecular dynamics has seen a surge of activity. Among others, most notably Car and Parrinello [1] have pioneered the version based upon density functional theory (DFT). This method has been applied to many systems, including, e.g. fullerenes [2] and polymers [3], and it has been extended to include gradient-corrected DFT [4] and self-interaction corrected DFT [5]. Its efficiency has been improved by several authors [6] by reformulating the DFT to scale only with system size, permitting much larger systems, and its theoretical background has been examined more thoroughly than before [7].

Also, non-DFT versions have received attention, albeit much less: Mohallem and co-workers [8] proposed fictitious dynamics as an alternative to the Roothaan procedure, with the nuclei held fixed. Ab initio Hartree–Fock self-consistent-field (HF-SCF) simulated annealing studies of small molecules were performed by Field [9]. Very recently, Hammes-Schiffer and Andersen [10] proposed an interesting variation of the theme: Based upon a "general HF"

theory, they speed up the computation by using analytically fitted ab initio matrix elements or semi-empirical potentials. However, this is clearly a departure from the ab initio path.

We have recently implemented ab initio molecular dynamics simulated annealing at the generalized valence bond (GVB) level (in the following called AIMDSA) and have used it for small-scale test calculations [11]. In this Letter, we want to show that our method permits applications to systems of non-trivial size, with transition metal atoms, and with non-trivial potential energy surface (PES) features.

For this purpose, we have chosen Ni_5 as an example. Nickel is continually receiving interest in surface reactivity and catalysis model reactions, see for example refs. [12,13]. For the particular case of Ni_5, there seemed to be some uncertainty in the literature in the past, regarding its structure: After semi-empirical calculations [14] had indicated a planar pentagon, Siegbahn and co-workers [15] suggested that Ni_5 has a planar "W"-structure, while recent CI calculations including d orbitals [16] point to a trigonal bipyramidal structure. Hence, we can expect a non-trivial PES at any sufficiently sophisticated level

of theory – and this is our only motivation. We neither want to solve nor add to the structural debate. This Letter serves to show the feasibility of AIMDSA on a transition metal PES with several important minima, and simultaneously to show limitations of our current AIMDSA technology. The moderate system size explored here still permits the more traditional way of geometry optimization, namely, using local optimization methods from selected starting geometries. This allows us to verify our AIMDSA result with local optimizations. We will show that AIMDSA gives the correct global minimum in one single run, independent of the starting conditions and of the propagation history. As discussed in detail in one of our previous publications [11], this feature is an essential advantage of simulated annealing approaches: They exhibit convergence towards the global minimum, while this is completely lacking in any approach using local optimization. Hence, simulated annealing approaches will be vastly superior in systems of larger size.

2. Calculational method

Our AIMDSA method and its implementation have already been described in detail in a previous publication [11]. For the present application system, we have chosen a double-zeta valence basis set and one-electron effective core potential, developed by Upton and Goddard [17]. The effects of the 3d orbitals are included in the effective core potential, and only one valence electron (4s) per nickel atom is described explicitly. Since nickel has the smallest d orbitals of any transition metal, it is the best candidate for this crude description that assumes the d electrons play no role in bonding. Siegbahn has used this model extensively to mimic nickel surfaces [18–20].

The five s electrons treated explicitly in this model for Ni_5 are coupled into a doublet spin eigenstate. This doublet state of Ni_5 is modeled at the GVB(2/4)-PP level, that is, in addition to the single open-shell orbital, the wave function contains two GVB pairs described by four natural orbitals. With 40 basis functions for five orbitals, we therefore have 200 SCF coefficients and four GVB CI coefficients in the electronic part of the AIMDSA propagation. In spite of the system size and the use of full forces, the computational effort is still manageable: On average, one propagation step takes 40 s CPU on an HP Apollo 9000 series 720 workstation.

In order to speed up the sampling of the potential surface via molecular dynamics [11], the masses of the nickel atoms are scaled down by a factor of five to the value 11.742 amu = 53492.6 au, while each SCF and GVB coefficient is assigned a fictitious mass of 300 au. The time step is 5 au (≈ 0.12 fs), but as before [11] we use a skipping/extrapolation scheme to speed up the calculation further: Integrals over basis functions are recalculated only at every fifth step, and the forces are recalculated at every tenth step with linear extrapolation in between. Error accumulation necessitates a traditional SCF-type reconvergence of the wave function every 100 steps (with the exception of the first 2000 steps, where the wave function is reconverged every 50 steps, due to the high velocity of the nuclei).

Simulated annealing is set into effect by scaling down the velocities of the nuclei by a factor of 0.9, in between 1000-step periods of free propagation. This schedule is held constant throughout the propagation. Random 3D geometries are generated as initial conditions, together with random velocities corresponding to 0.0475 hartree total nuclear kinetic energy (approximately 2000 K instantaneous temperature). The initial conditions have zero total linear and angular momenta, which is preserved during the propagation. A spherical, reflecting boundary with a radius of 6 Å around the center of mass prevents dissociation at high temperatures.

3. Results

We will show AIMDSA propagations for two entirely different initial conditions: Both are random 3D structures, but the potential energy of structure A is 0.048 hartree above the final "W"-structure (see below), while structure B is at 0.166 hartree above the final structure. Both initial conditions were propagated as described above, and cooled down until the nuclear kinetic energy was of the order of 0.005 hartree (210 K instantaneous temperature) and until visual inspection of the movement of the nuclei

showed trapping of the system in one well-defined basin of attraction.

Fig. 1 depicts the development of the potential energy of the Ni_5 system during both propagations (with initial structures A and B, respectively); representative snapshots of the nuclear geometry are shown in fig. 2. For structure A, the geometry optimization proceeds in three distinct stages: In the first third of the propagation (characterized by high-amplitude, low-frequency oscillations of the potential energy value), the system samples different 3D arrangements, in the middle third it has settled down to more or less planar structures (the oscillations of the potential energy now are very irregular and have lower amplitude, but higher frequency), which freeze out to one preferred structure in the last third (with typical smooth, regular, low-frequency oscillations of the potential energy, corresponding to residual vibrations around a single minimum). The AIMDSA propagation of structure B shows similar stages in its latter half, while the first half constitutes an addi-
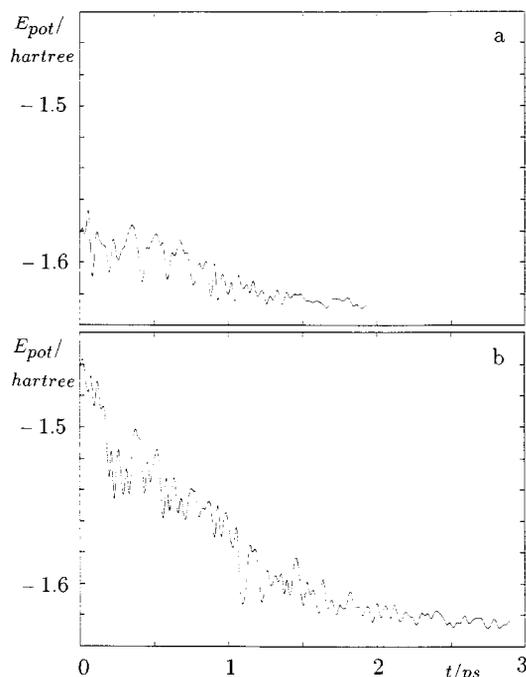
tional state: The energy is above the $Ni_3 + Ni_2$ dissociation limit and therefore the system tries to move from the initial conditions directly to dissociation, but this is prevented by reflection of one atom from the spherical boundary. Note that in both instances the system finally arrives at the same structure, despite the totally different propagation histories.

Fig. 3 shows the total energy of Ni_5 during optimization of structure B. The regular steps indicate the external cooling according to the cooling schedule. In between these steps, the curve should be perfectly flat in free, physical dynamics, indicating conservation of total energy. Instead, wiggles of low amplitude and a slight decrease can be observed here, particularly at early times. This is an indication of an additional energy loss beyond the intended cooling schedule: Every 100 steps the wave function is reconverged, resulting in both the SCF and GVB coefficients being reset to values appropriate to the instantaneous nuclear positions, irrespective of the previous (fictitious) kinetic energy content of the coefficients. Since there is in general a transfer of kinetic energy from the real degrees of freedom (the system of the nuclei) to the more numerous fictitious degrees of freedom (the wave function coefficients), the wave function reconvergence constitutes a drain of kinetic energy. With further increases in the number of orbitals and GVB pairs in the systems this effect can become dominant (e.g., in Si_4 or Si_6, see ref. [21]), making introduction of thermostating devices for the real and fictitious systems necessary [21,22]. In the present case, however, the explicit cooling schedule steps still dominate, and hence a controlled cooling is possible.

Any geometry sampled during the last few hundred steps of either of the two propagations yields the exact same final structure upon subjection to a traditional, local geometry optimization procedure: the "W"-like form of C_{2v} symmetry already shown in fig. 2. It is perfectly planar, the Ni–Ni nearest neighbor distances are between 2.26 and 2.28 Å, and the potential energy is −1.630678 hartree (this is the zero of energy referred to above). Experimental Ni–Ni distances are 2.49 Å in bulk nickel and 2.2 Å in Ni_2. Other likely candidates for the global minimum are the trigonal bipyramid and the pentagon. At this level of theory, the trigonal bipyramid is Jahn–Teller distorted and has an energy of −1.619971 hartree, while

Fig. 1. Temporal behavior of the potential energy (electronic energy plus internuclear repulsion) of Ni_5 during simulated annealing trajectories A (panel (a)) and B (panel (b)).
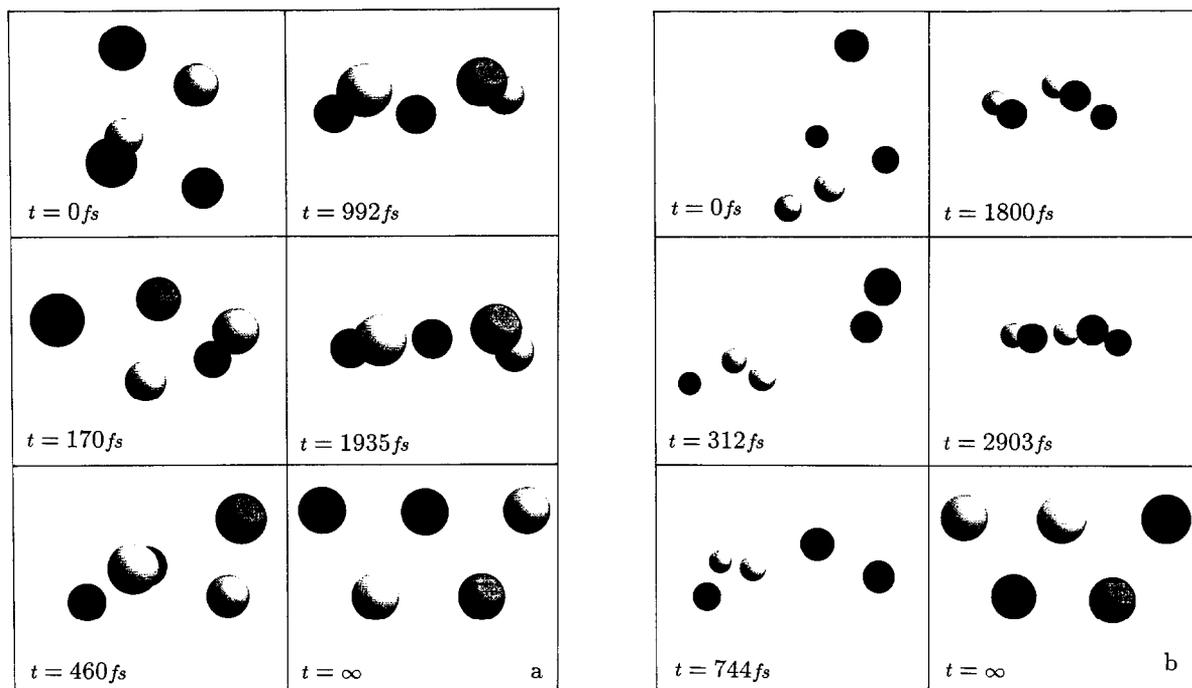
Fig. 2. Snapshots of the nuclear dynamics during simulated annealing of Ni_5, for trajectories A (panel (a)) and B (panel (b)). In the pseudo-3D rendering of the cluster, larger circles denote atoms closer to the viewer, while those farther away appear smaller. Different shadings of the atoms are for identification purposes. For both trajectories, the initial and final geometries as well as three intermediate geometries are shown, all from the same perspective. Time "infinity" refers to the result of a traditional, local optimization of the final geometry of each trajectory, shown from a different perspective for clarity; these geometries are identical for cases A and B.
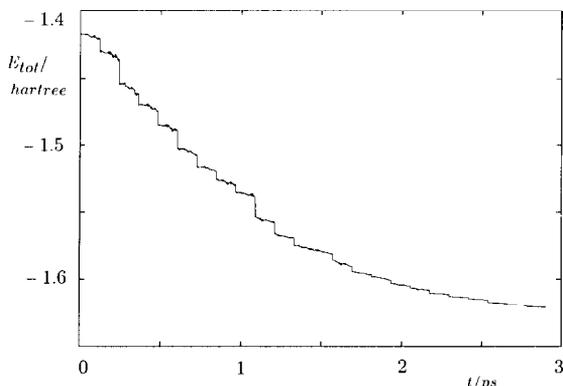

Fig. 3. Temporal behavior of the total energy of Ni_5 (kinetic energy of real plus fictitious degrees of freedom, plus potential energy) for trajectory B (trajectory A exhibits similar characteristics). The regular steps indicate cooling according to the cooling schedule; remaining deviations from a constant value point to partial energy loss, see text for details.

the pentagon appears not to be a minimum at all: All attempts to optimize the geometry of pentagonal and near-pentagonal starting geometries with a traditional, local optimization procedure yielded the same "W"-structure as above. Therefore, it is very likely that AIMDSA discovered the true global minimum in both propagations, i.e. independent of the starting geometry. Again, we would like to emphasize that the level of theory used here is clearly deficient (no explicit treatment of d orbitals, only a small-scale CI treatment). We are not trying to find the lowest-energy configuration of Ni_5 with the best electronic structure theory available; instead, we are trying to demonstrate the strengths and weaknesses of the GVB-AIMDSA approach on a PES of realistic complexity.

4. Conclusions

We have demonstrated the feasibility of AIMDSA for a small transition metal cluster with a non-trivial PES. As demonstrated with two entirely different AIMDSA propagations ending up in the same structure, and with supplementary traditional, local optimizations, we have most likely found the global minimum at this particular level of theory. The computational effort is not small, but also not prohibitive; calculations of the size presented here can easily be performed on fast workstations.

Application to systems with more orbitals and GVB pairs [21] will require special measures against disruption of the cooling schedule by energy loss through the fictitious degrees of freedom. Future work on the GVB level will also include the multiple time scale technology introduced previously [23,24].

References

[1] R. Car and M. Parrinello, Phys. Rev. Letters 55 (1985) 2471.

[2] W. Andreoni, F. Gygi and M. Parrinello, Chem. Phys. Letters 190 (1992) 159.

[3] G. Brocks, P.J. Kelly and R. Car, Synth. Metals 57 (1993) 4243.

[4] K. Laasonen, M. Parrinello, R. Car, C.Y. Lee and D. Vanderbilt, Chem. Phys. Letters 207 (1993) 208.

[5] E.S. Fois, J.I. Penman and P.A. Madden, J. Chem. Phys. 98 (1993) 6352.

[6] M. Pearson, E. Smargiassi and P.A. Madden, J. Phys. Condens. Matter 5 (1993) 3221;
F. Mauri, G. Galli and R. Car, Phys. Rev. B 47 (1993) 9973;
G. Galli and M. Parrinello, Phys. Rev. Letters 69 (1992) 3547.

[7] E.S. Kryachko, Phys. Rev. B 47 (1993) 15935; J. Phys. Condens. Matter 5 (1993) 4429.

[8] R.O. Vianna, H. Chacham and J.R. Mohallem, J. Chem. Phys. 98 (1993) 6395.

[9] M.J. Field, J. Phys. Chem. 95 (1991) 5104.

[10] S. Hammes-Schiffer and H.C. Andersen, J. Chem. Phys. 99 (1993) 523, 1901.

[11] B. Hartke and E.A. Carter, J. Chem. Phys. 97 (1992) 6569.

[12] I. Panas, P. Siegbahn and U. Wahlgren, J. Chem. Phys. 90 (1989) 6791;
P.E.M. Siegbahn, M.R.A. Blomberg and C.W. Bauschlicher Jr., J. Chem. Phys. 81 (1984) 2103.

[13] R. Fournier, J. Andzelm, A. Goursot, N. Russo and D.R. Salahub, J. Chem. Phys. 93 (1990) 2919.

[14] J. Koutecký and P. Fantucci, Chem. Rev. 86 (1986) 539.

[15] M.A. Nygren, P.E.M. Siegbahn, U. Wahlgren and H. Åkeby, J. Phys. Chem. 96 (1992) 3633.

[16] V. Bonačić-Koutecký, private communication.

[17] T.H. Upton and W.A. Goddard III, CRC Critical Rev. Solid State Mater. Sci. 10 (1981) 261.

[18] I. Panas, J. Schüle, P. Siegbahn and U. Wahlgren, Chem. Phys. Letters 149 (1988) 265.

[19] I. Panas, P. Siegbahn and U. Walgren, in: The challenge of d and f electrons: theory and computation, eds. D.R. Salahub and M.C. Zerner, ACS Symp. Ser. No. 394, ch. 9.

[20] I. Panas, P. Siegbahn and U. Wahlgren, Theoret. Chim. Acta 74 (1988) 167.

[21] B. Hartke, D.A. Gibson and E.A. Carter, in preparation.

[22] I. Stich, R. Car and M. Parrinello, Phys. Rev. Letters 63 (1989) 2240;
P.E. Blöchl and M. Parrinello, Phys. Rev. B 45 (1992) 9413.

[23] B. Hartke, D.A. Gibson and E.A. Carter, Intern. J. Quantum Chem. 45 (1993) 59.

[24] D.A. Gibson and E.A. Carter, J. Phys. Chem., submitted for publication.